Experimental Investigation of Stochastic Pulsation and Formation of Light Bullets with Megagauss Magnetic Fields by an Intense Laser Pulse Propagating in a Preionized Plasma

Nadja I. Vogel and N. Kochan

University of Technology Chemnitz, Department of Physics, Optical Spectroscopy and Molecule Physics, 09107 Chemnitz, Germany

(Received 25 July 2000)

The generation of extremely stable light bullets in a preformed plasma near critical density has been observed experimentally during the interaction of intense picosecond laser beam with a metallic target in air. Optical probing measurements indicate the formation of pulsating channels, typically of about 5 μm in diameter, directed towards a heating laser beam, as well as of disconnected massive plasma blocks moving also towards the laser beam. The velocities of the dense plasma blocks reach the values of 4.5×10^8 cm/s. The blocks are stable during their acceleration and propagation in air. Self-generated magnetic fields up to 4–7 MG were observed by means of the Faraday rotation of a probe laser beam.

DOI: 10.1103/PhysRevLett.86.232 PACS numbers: 52.38.–r, 52.35.Mw, 52.35.Tc, 52.70.–m

Laser-plasma interaction for moderate intensities of laser radiation (10^{13}–10^{15} W/cm^2) showed filamentation and formation of jets the diameter of which is substantially smaller than the spot diameter of the incident laser beam [1–4]. Apart from the lateral effects, a very complex temporal stochastic pulsation with a period of about 10 to 50 ps was reported in [5–7]. In a numerical hydrodynamic study [8] it has also been shown that generation of fast moving plasma blocks with velocities beyond 10^8 cm/s is possible due to ponderomotive force in a plasma layer near the critical density. In this paper we report the first interferometric observations of the dynamics of light bullets, accelerated thick plasma blocks, generated in air during the interaction of a picosecond laser pulse with an Al target at irradiances of 10^{14} W/cm^2, as well as of a periodical (10–40 ps) self-channeling of laser beam in narrow plasma channels in front of the surface of strong shock waves. High density blocks of plasma move with velocities of about $(2–4.5) \times 10^8$ cm/s towards the laser beam and keep a stable configuration in space and time during the laser pulse. The effect is strongly resonant; the accelerated plasma blocks appear only when the laser pulse energy exceeds 60 mJ (for the pulse duration of 100 ps and the beam wavelength $\lambda = 1064$ nm). The interaction results then in a strong increasing of the ponderomotive force and in a growth of the associated nonlinear phenomena. For Faraday-rotation and interferometric measurements of spatial profiles of the self-generated magnetic fields in all the investigated plasma objects a second-harmonic probe beam was used. An intense horizontally polarized IR pulse (100 mJ, 100 ps, 1064 nm) from the Nd:YAG laser was focused by a 25 cm focal length lens to the maximum intensity of 8×10^{13} W/cm^2. The laser beam was incident normal on the planar Al target in air. The target was placed in one arm of the Michelson interferometer. The probing laser beam at the second harmonic ($\lambda = 532$ nm) was optically delayed from -2 to 10 ns with respect to the ignition beam. Imaging of the target and of the focal region of the laser pulse with the resolution of 1 μm was achieved by means of the long-distance microscope Questar 100 placed at a working distance of 10 cm. Interferometric and shadowgraphic measurements of the laser-produced plasma were carried out in parallel with polarimetric measurements. By taking into account the axial symmetry of the investigated plasma, it was possible to reconstruct the distribution of the magnetic induction vector $B(r, z)$ for different delay times relative to the laser pulse.

A significant feature of our experimental setup is the amplified spontaneous emission (ASE) arising in long intensity pedestal (ns range). The value of the contrast of laser radiation in the main peak to the pedestal radiation is 150 only, so the intensity in the prepulse was about 5×10^{11} W/cm^2, which is well above the generally accepted long pulse threshold intensity for plasma generation in air. By focusing the heating laser beam to the spot size of 30 μm in front of the target, it was possible to form a low density plasma before the main pulse with $I = 8 \times 10^{13}$ W/cm^2 reached this region. It is evident from Fig. 1, in which the time history of the propagation of a horizontally polarized laser pulse (energy 100 mJ, pulse duration 100 ps, and wavelength $\lambda = 1064$ nm) is shown. The times indicated at each image in Fig. 1 correspond to the time delay between the probe pulse and the center of the heating beam. The shadowgrams clearly show a shock wave front with a steep density gradient, which is formed $\sim$2 ns before the pulse center of the heating beam reaches this point. The electron density in front of the shock wave determined from interferogram is of the order of 10^{20} cm^{-3}, the front width being about 5 μm. Strong absorption of laser radiation in this thin plasma layer is witnessed by a characteristic plasma emission at the second harmonic of laser frequency. In the shadowgram recorded at $t = -700$ ps [Fig. 1(a)] the $2\omega_0$ emission

 0031-9007/01/86(2)/232(4)$15.00

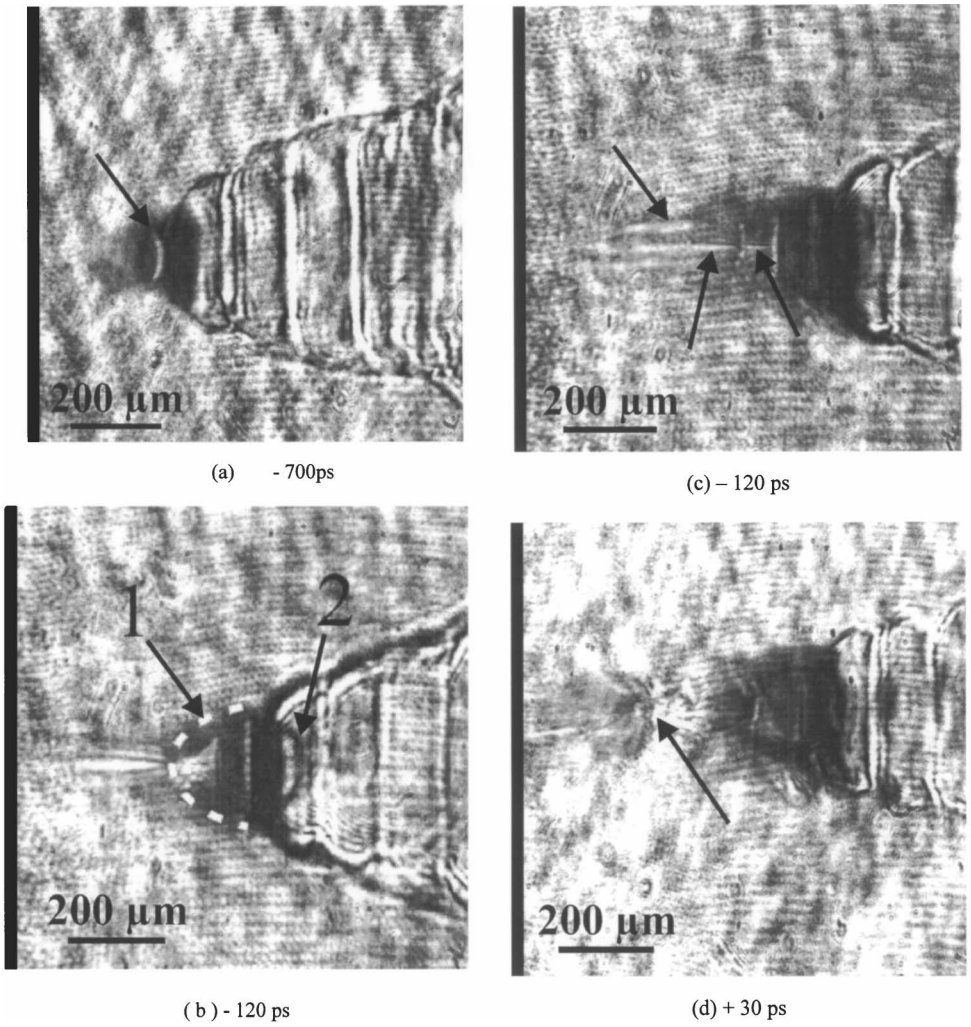

FIG. 1. Shadowgrams showing the time history of laser beam interaction with the preformed plasmas for propagation of 100 mJ laser pulse (from left) in air near the Al target (right). Delay times between the probe pulse at 532 nm and heating beam at 1064 nm are indicated below each image. (a) Self-emission at 2ω marked by arrow assigns a resonance absorption surface. (b) Arrows marked 1 and 2 show oppositely directed shock wave fronts. Self-focusing of laser beam to filaments of 5 μm diameter is evident in front of shock waves (left). (c) Filament formations in front of shock waves are shown by arrows. (d) Arrows indicate the moment of plasma block disruption.

in the form of a concave disk with the diameter of 50 μm is clearly visible. This is the region where the incident laser frequency ω_0 equals the plasma frequency ω_p and the conditions for resonant absorption are fulfilled. For the s-polarized laser heating pulse in the case of oblique incidence the position of the cutoff occurs at the point where $\omega_p = \omega_0 \cos\theta$. By taking $\cos\theta = 0.3$ from Fig. 1(a), we obtain $N_e = 1.2 \times 10^{20}$ cm^{-3}, which is in good agreement with the interferometric plasma density measurements. When the leading part of the heating pulse penetrates the plasma with such a density gradient, a narrow filament about 5 μm in diameter and 200–300 μm long accompanied with strong shock waves appears [Figs. 1(b) and 1(c)]. One shock wave (2) propagates with the velocity of 6×10^7 cm/s towards the target [its front 2 is clearly visible in Fig. 1(b)], and another one (1) in the opposite direction, towards the heating laser beam, with $V = 2.25 \times 10^8$ cm/s. It should be noted that the filaments are formed in front of the shock waves displaced, one with respect to another, by $\Delta l \sim 30$–50 μm [Fig. 1(c)]. When taking into account that filaments are formed during the heating pulse and each shadowgram gives a frozen 100 ps snapshot of the interaction, then the average pulsating time of filaments can be calculated as $t = \Delta l/V = 13$–22 ps.

Besides the filamentation, for later delay times we have observed accelerated massive plasma blocks (fragments) moving towards the heating beam. These plasma fragments retain the concave-convex configuration of the resonance absorption layer. In some cases, the boundary in the abrupt pulled off fragments is not smooth, its outline copying exactly the boundary in the remaining plasma body. Figure 1(d) illustrates the moment of disruption of a plasma fragment from the plasma body, while the moving off plasma blocks—"light bullets"—are well seen in Fig. 2. Close the point of disruption, a shock wave structure with Mach whiskers typical for a hydrodynamic blow was observed. For later delay times

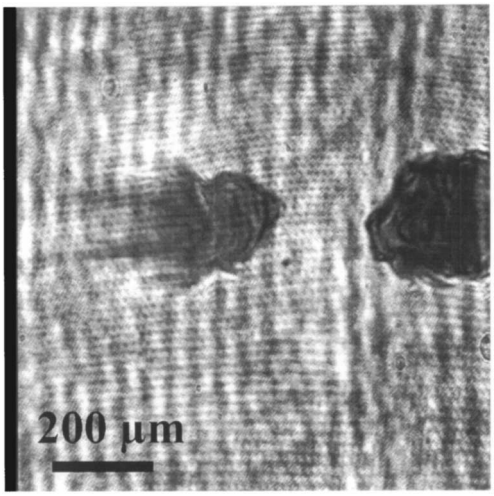

FIG. 2. Shadowgram showing the "light bullets" for delay time $t = 60$ ps. Laser beam is incident from the left.

($t = 400-1000$ ps) the shock wave fronts extinguish again. From many series of such shadowgrams it was possible to estimate the average velocity and the acceleration of the moving plasma blocks, $(3.3 \pm 1.3) \times 10^8$ cm/s and $(7 \pm 3) \times 10^{18}$ cm/s^2, respectively. As all the data are time integrated over the 100-psec laser pulses used, the maximum instantaneous velocity and acceleration values may be even higher. The large magnetic fields associated with resonant absorption in the plasma near the surface of critical density have been studied with the Faraday-rotation diagnostic system for the probe-beam timing $t = -60$ ps, 0 ps, +60 ps, +120 ps, +200 ps.

The Faraday rotation of the probing light appeared as early as −60 ps, reached its maximum near +60 ps, and then decreased again (it could be seen as late as +200 ps). The results obtained for probe-beam timing of +60 ps are shown in Fig. 3. Each photograph shows the actual orientation of plasma target with plasma blocks near the surface of the shock wave front (with the main laser pulse incident from the left). The well-localized thin bright stripes above and below the center of the plasma block are evident. The reversal of the analyzer orientation produces always a corresponding reversal in the position of the bright stripes. Opposite to the thermally generated magnetic fields the orientation of azimuthal magnetic field in plasma blocks is found to be consistent with the direction of the current flow driven by a ponderomotive force along the resonance absorption surface [9,10]. The magnetic field orientation and the current flow lines are shown schematically in Fig. 4. The azimuthal direction remained unchanged throughout the observation interval (−60 ps to +200 ps) and the magnetic field lines were frozen in the moving massive plasma blocks. We estimate a typical rotation angle to be about 0.4–0.6 rad. By using electron density distribution determined by Abel inversion of interferograms [see Figs. 5(a) and 5(b)] and assuming that the magnetic field varies inversely as the radial position in plasma blocks, we can calculate the magnetic field magnitude required for this

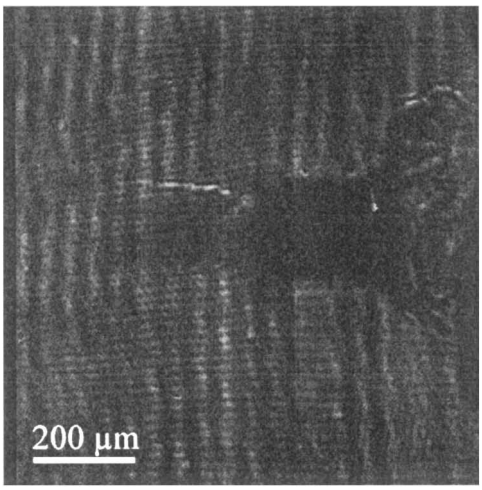

(a) - 25°

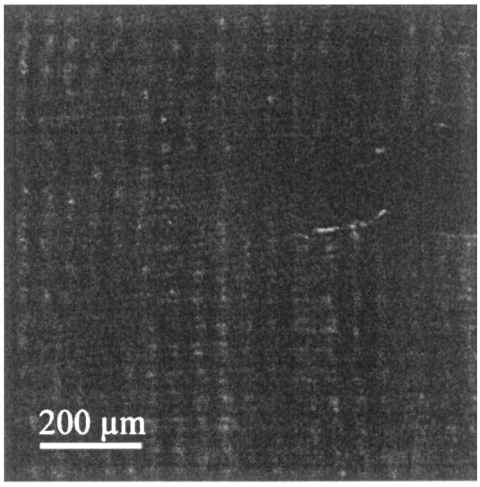

(b) +25°

FIG. 3. Faraday-rotation photographs for probe-pulsing timing $t = 60$ ps. View into probing beam with main laser beam incident from the left. Analyzer orientation (with respect to the crossed position) is shown below each photograph and taken as positive when clockwise. The position of rotated light (bright stripes) reverses with reversal of analyzer orientation.

Faraday rotation angle. The calculated average values of magnetic field are of order 4–7 MG.

The physical mechanism for the generation of the observed high dc magnetic field is quite simple. The magnetic field is generated by dc currents driven by the ponderomotive force of the laser pulse within the skin layer where resonance absorption of laser light occurs. It follows from high values of magnetic fields (4–7 MG) observed in our experiments, as well as from the structure of measured magnetic fields, which arise within the plasma layer and are oppositely directed to the thermoelectric fields. According to the plasma target geometry in our experiments [Fig. 1(a)] the *s*-polarized incident beam is not strongly normal to the cutoff plasma surface, and there is a component of the incident electric field (tangential component) along the resonance absorption

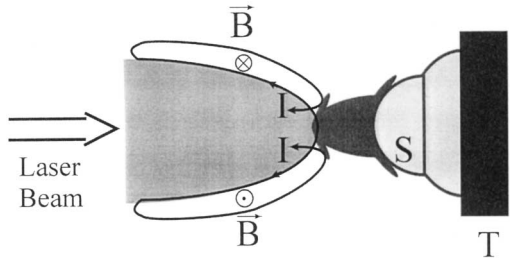

FIG. 4. Schematic showing the target surface (T), the shock waves (S), the orientation of dc magnetic field (**B**) within the skin layer at the plasma-air interface, and the lines of current flow giving rise to **B**.

surface which drives electrons in the skin layer. Theory predicts the growth of dc magnetic fields due to resonance absorption by approximately the rate of 6 MG/psec [10], which is in reasonable agreement with the measured values (4–7 MG).

The physical mechanism for blowing off of the massive plasma blocks outwardly from the resonance absorption layer may originate from a magnetic ponderomotive force arising if a strong magnetic field is generated along the concave-convex surface of the resonance absorption layer. Lines of the current flow which gives rise to the dc magnetic field are shown schematically in Fig. 4. The force exerted by the magnetic field on the volume unit of a plasma block is given by $\mathbf{f} = N_e e[\mathbf{V_e} \times \mathbf{H}]/c = [\mathbf{J} \times \mathbf{H}]/c$.

The magnetic ponderomotive force is perpendicular to the plane $[\mathbf{J} \times \mathbf{H}]$. It is directed inwards and has a blowing effect on the plasma block. The high density moving plasma bullets observed in our experiments are likely due to this effect. The frozen magnetic fields in the plasma blocks keep them highly collimated.

In conclusion, we have demonstrated that the resonance absorption occurring near the shock wave front at the interaction of an intense laser pulse with a dense plasma is accompanied by generation of a strong dc magnetic field and by blowing off massive plasma blocks due to magnetic ponderomotive force. Though the effect described above was investigated with a tabletop device in the laboratory, it is very similar to the generation of energetic outflow of gas from astrophysical objects, e.g., the young stellar objects [11], in which strong magnetic fields at a great distance from the source have been observed. The outflows also are highly collimated and asymmetric [12]; the radio emission from a number of outflows is nonthermal [13]. Similar to the astrophysical jets, the crossing of current lines at $r = 0$ at the surface of resonance absorption observed in our experiments can lead to the crossing of magnetic field lines and to the explosive disruption of massive plasma blocks from the plasma body. The process is accompanied by a significant dissipation of power within the absorption layer. At the same time, the outflows of plasma convect the magnetic flux outwards.

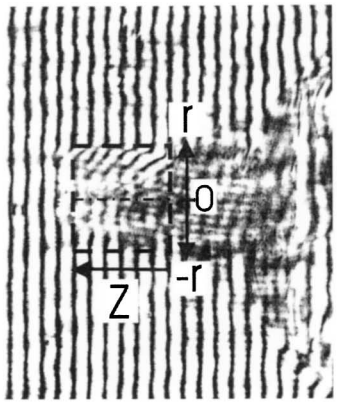

(a)

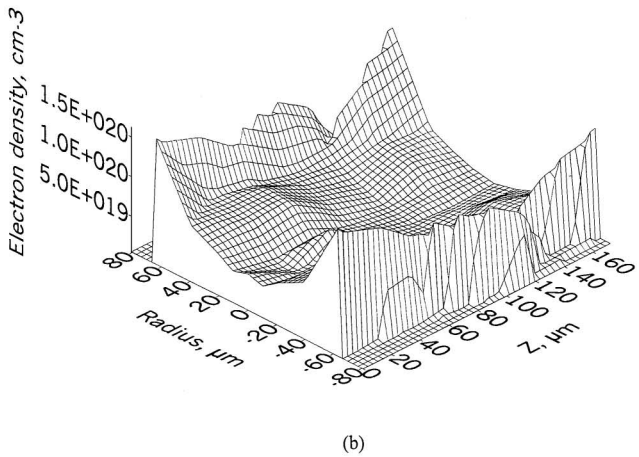

(b)

FIG. 5. Interferogram (a) and electron density distribution (b) for probe-pulse timing $t = +60$ ps.

[1] M. J. Herbst, J. A. Stamper, R. R. Whitlock, R. H. Lehmberg, and B. H. Ripin, Phys. Rev. Lett. **46**, 328 (1981).
[2] C. Joshi *et al.,* Opt. Commun. **70**, 44 (1989).
[3] N. G. Basov *et al.,* Pis'ma Zh. Eksp. Teor. Fiz. **38**, 60 (1983) [JETP Lett. **37**, 134 (1983)].
[4] N. E. Andreev, V. L. Arzimovich, V. T. Kasjanov, and V. T. Tichonchuk, Zh. Eksp. Teor. Fiz. **98**, 881 (1990) [Sov. Phys. JETP **71**, 490 (1990)].
[5] S. Jackel, B. Barry, and M. Lubin, Phys. Rev. Lett. **37**, 95 (1976).
[6] R. A. M. Maddever, B. Luther-Davies, and R. Dragila, Phys. Rev. A **41**, 2154 (1990).
[7] R. F. Turner, D. W. Phillion, E. M. Campbell, and K. G. Estabrook, Phys. Fluids **26**, 579 (1983).
[8] H. Hora, *Plasmas at High Temperature and Density* (Springer, Heidelberg, 1991), p. 204.
[9] R. N. Sudan, Phys. Rev. Lett. **70**, 3075 (1993).
[10] J. J. Thomson, C. E. Max, and K. Estabrook, Phys. Rev. Lett. **35**, 663 (1975).
[11] T. P. Ray, T. W. B. Muxlow, D. J. Axon, A. Brown, D. Corcoran, J. Dyson, and R. Mundt, Nature (London) **385**, 415 (1997).
[12] Bo Reipurth, John Bally, Robert A. Fesen, and David Devine, Nature (London) **396**, 343 (1998).
[13] S. Curiel, L. F. Rodriguez, J. Moran, and M. Canto, J. Astrophys. **415**, 191 (1993).